THE JOURNAL OF PHYSICAL CHEMISTRY C

ARTICLE

pubs.acs.org/JPCC

Dopant Effects on Single and Multiple Excitons in Small Si Clusters: High-Level Ab Initio Calculations

Sean A. Fischer[†] and Oleg V. Prezhdo[‡,*]

[†]Department of Chemistry, University of Washington, Seattle, Washington 98195, United States

[‡]Department of Chemistry, University of Rochester, Rochester, New York 14627, United States

ABSTRACT: Doping has been critical to the realization of current semiconductor devices, allowing for control and tuning of the electronic properties. Whereas doping is now common in bulk, its extension to spatially confined materials has not been easy. Recently, suitable synthetic methods have been developed, and it has become vital to understand the changes doping affects in spatially confined materials. For this purpose, we performed high-level, ab initio quantum-chemical calculations on small boron- and phosphorus-doped Si clusters, and obtained optical absorption spectra and excited states properties over a broad energy range, including single and multiple excitons. We find that doping blue-shifts the optical absorption spectra and moves the onset of multiexciton configurations to significantly higher energies. The latter factor can be very important in photovoltaic applications. The effect of doping on the cluster properties is similar to that of charging.

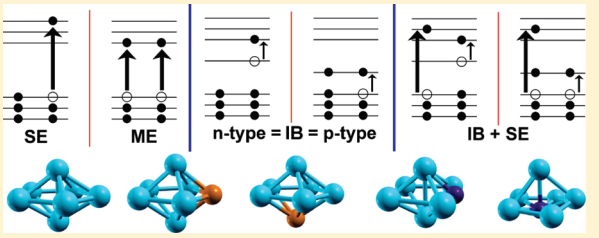

1. INTRODUCTION

For years, dopant atoms have been added to semiconducting materials to endow new properties to the system or to enhance those properties already present. In bulk semiconductors, doping is common and well understood; however, the same cannot be said of spatially confined versions of these materials. The smaller size of systems in the quantum confinement regime intrinsically makes the lowest doping concentrations orders of magnitude larger than those of even heavily doped bulk materials.[1] In addition, dopant effects may not follow the bulk trends, given that undoped quantum confined materials already exhibit unique optical and electronic properties.[2]

Generally, doping of nanoscale clusters presents a synthetic challenge.[3] Defect formation energies grow, as the size of the nanocrystal (NC) decreases, resulting in pronounced self-purification of small to medium sized clusters.[4] Calculations show that, below a critical crystal size, it is energetically favorable to eject dopant atoms to the surface.[5] Recent synthetic successes include II−IV semiconductors doped with transitions metals such as Mn[6,7] producing novel magnetic materials,[8−10] and the creation of n- and p-type materials via either charging[11−13] or heterovalent impurity doping.[14,15] It is this last type of doping with which the present work is concerned. Whereas some optical and transport properties of doped NCs have been elucidated,[16] there has been little research devoted to the characterization of excited states in these materials.

Impurity doping creates defect states that lie close in energy to either the valence band (VB) or conduction band (CB), depending on whether electron acceptor or donor impurities are introduced. In larger clusters, the energy of the defect level is independent of cluster size.[17,18] Charge carriers in these defect states become activated, either thermally or through confinement effects,[16] and act as free carriers, leading to the drastic increase in conductivity in the semiconductor. It was already demonstrated[19,20] that an extra charge carrier introduced into either the VB or CB through charging has a very significant effect on the excitations and optical spectra of small semiconducting clusters. It is important to elucidate whether or not the heterovalent impurity doping has a similar effect.

A priori, one may expect notable differences between charging and heterovalent doping, in particular because the latter creates much more localized states, lowers the bandgap, and distorts the geometric structure of the cluster. In the case of a single dopant atom, the defect state is partially occupied, creating the possibility that an excitation in the system will not produce an exciton, but rather will induce a transition of the intraband (IB) type. This situation is shown diagrammatically in Figure 1, along with the other possible excited state configurations. Opening up the IB excitation channel could impact the energies at which pure single exciton (SE) and multiple exciton (ME) configurations are seen. As a result, applications that utilize doped semiconductors and rely on electronic excitations can be significantly affected.

In this article, we gain insight into the effects of heterovalent dopants on the energies, optical activity, and single-particle origin of electronic excitations in small semiconductor clusters. We perform high-level ab initio quantum-chemical calculations over a broad range of energies and excitation types. In particular, we investigate several hundred lowest excited states of small silicon clusters that have been doped with either a boron or a phosphorus atom and compare the results with those for the undoped

Received: March 15, 2011
Revised: April 12, 2011
Published: April 29, 2011

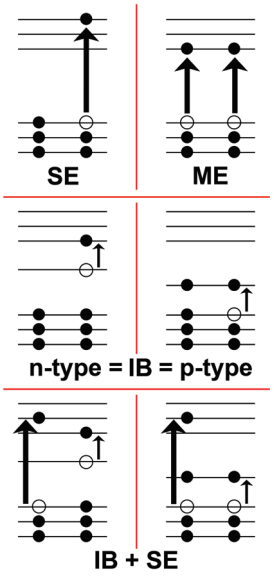

Figure 1. Types of transitions that are possible in the studied systems. SE and ME refer to single exciton and multiexciton respectively, whereas n-type and p-type refer to intraband (IB) transitions that become possible when the cluster is doped. Combinations of IB and SE transitions can occur as indicated at the bottom. IB + ME transitions are also possible.

cluster. Similar to direct charging, heterovalent doping creates dramatic changes in the cluster properties. New excitations appear at low energies; however, these transitions exhibit weak optical activity. SEs shift to higher energies and cover a broader energy range. Because SEs exhibit highest optical activity, the electronic adsorption spectrum blue-shifts. ME transitions appear at energies that are almost twice higher in doped than undoped clusters. Mixed IB + SE transitions, involving excitation of the dopant state along with excitation across the fundamental bandgap, slightly precede MEs in energy, but generally appear within the same energy range as MEs. The effects of doping on the nature and optical activity of electronically excited states in the small silicon clusters are essentially independent of the position of the dopant atom and whether the doping is n- or p-type.

The paper is constructed as follows. The Theory section introduces the basics of the high-level ab initio electronic structure approach and presents the technical aspects of the calculation. Next, the geometry, optical absorption spectra and single particle origin of the electronic excitations in pristine, n- and p-doped Si clusters are discussed in detail. The paper concludes with a summary of the key findings and their implications for ME generation (MEG) in semiconducting NCs.

2. THEORY

The study was performed using the symmetry adapted cluster theory with configuration interaction (SAC−CI)[21,22] as implemented within the *Gaussian 03* computational package.[23] SAC−CI is an advanced quantum-chemical methodology that includes electron correlation effects for both ground and excited electronic states, thereby providing a very high-level description of electronic excitations with explicit account for the Coulomb interaction between electrons and holes. It starts at the single-particle level and explicitly includes electron correlation effects through the cluster expansion of the ground state wave function:

$$|\Psi^{SAC}\rangle = \exp\left(\sum_{I=1}^{M} C_I \hat{S}_I\right)|\Phi_0\rangle = \left(1 + \sum_I C_I \hat{S}_I + \frac{1}{2}\sum_{I,J} C_I C_J \hat{S}_I \hat{S}_J + \ldots\right)|\Phi_0\rangle \quad (1)$$

Here, $|\Phi_0\rangle$ represents the closed-shell Hartree−Fock (HF) determinant, S_I are symmetry adapted excitation operators, and C_I are variable coefficients. This SAC expansion dramatically improves the description of the ground state relative to the HF level. Electronic excitations are obtained by application of high-order excitation operators to the correlated ground state. The excited state wave functions $|\Psi^{SAC-CI}\rangle$ are calculated from the electron correlated ground state wave function $|\Psi^{SAC}\rangle$

$$|\Psi^{SAC-CI}\rangle = \sum_{K=1}^{N} d_K R_K |\Psi^{SAC}\rangle \quad (2)$$

where R_K represents an excitation operator, and d_K is the SAC−CI coefficient. For the calculations discussed here, excitation operators up to at least quadruples were utilized. The excited states can then be classified according to the types of transitions that comprise each excited state, including single, double, triple, quadruple excitations, and so on.

The SAC−CI method is different from other approaches, such as the linear response time-dependent (TD) HF or density functional theory (DFT). Standard linear response TDHF and TDDFT remain within the single-particle picture and do not produce states with ME character.[24,25] SAC−CI goes beyond the modeling of single excitations, thereby allowing us to qualify the excited states as single or MEs.[22] Potentially, real-time and nonadiabatic TDDFT can model both single and multiple excitations.[26−29] However, it is still a state-of-the-art technique that it is not routinely available in electronic structure packages. Real-time TDDFT is significantly more computationally expensive than linear response TDDFT. For comparison, linear response TDDFT spectra were computed as well.

As a consequence of the complexity of the calculation and the supremely large number of states needed to span a meaningful energy range, rather small clusters of atoms have to be used. Previous results[19,20,30] supported by analytic theory[31] suggest that these small clusters provide data that are at least qualitatively applicable to the larger NCs.

The cluster geometries were optimized using the B3LYP density functional, the LANL2DZ basis set and pseudopotentials representing the core electrons. The geometry of the pristine Si_7 cluster was constrained to have the D_{5h} symmetry. The geometries of the doped clusters were optimized under the correspondingly lowered symmetry constraints. Then, the energies, oscillator strengths, and single-particle orbital origins of the electronically excited states were calculated. All occupied and virtual orbitals were included in the SAC−CI active space. Excitations up to quadruples were obtained; however, the contribution of excitations involving more than 2 electrons was minimal, never reaching above 5%.

The study focuses on the Si_7 cluster doped with either a phosphorus or a boron atom at two different locations. The energy is shown in units of the lowest excitation energy, that is the gap energy E_g = 2.6 eV, of the pristine Si_7 cluster, as commonly done in QD literature.[32−36] The energy range in the

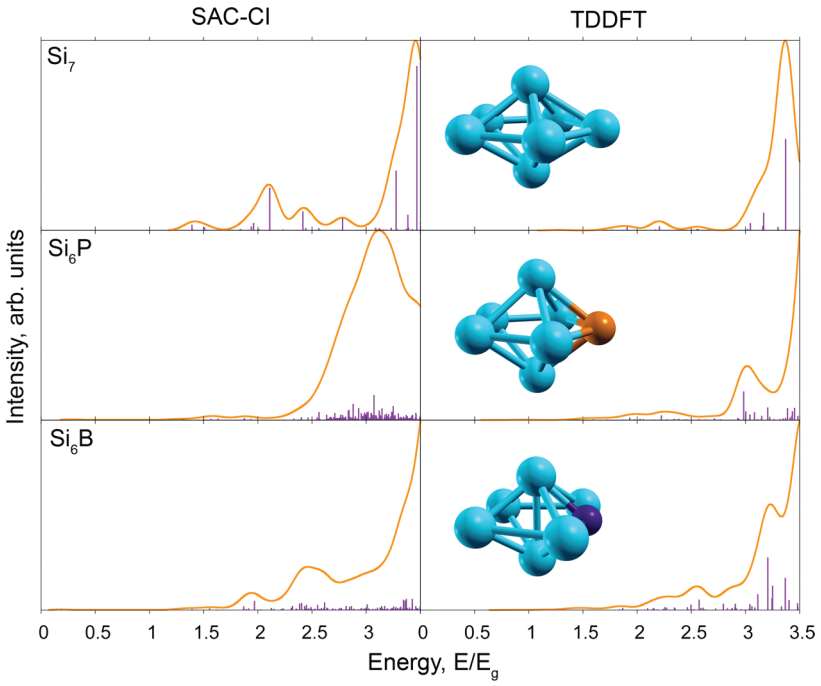

Figure 2. Calculated optical absorption spectra of undoped and doped Si clusters. Inserts show the optimized geometries.

figures considered below extends up to 9 eV, which is close to the ionization potential of the Si atom. DFT calculations using a basis set that is larger than LANL2DZ used here predict the ionization potential of the Si_7 cluster at slightly above 8 eV, as seen in Figure 4 of ref 37. Our SAC−CI/LANL2DZ calculation gives the ionization potential of Si_7 at 8.9 eV. This value is slightly overestimated due to the moderate size of the basis set. Increasing the basis would make SAC−CI calculations prohibitively expensive. It should be noted that, in comparison with our work, no other publication treats so many singly and multiply excited states in QD clusters of any size at an equivalent ab initio level.

3. RESULTS AND DISCUSSION

The geometries of the pristine Si cluster and the clusters doped in the equatorial plane are displayed in Figure 2. As would be expected, replacement of a Si atom with a P atom has a minor effect on the geometry of the cluster, because Si and P belong to the same row in the periodic table of elements and have similar sizes. The P atom sits slightly closer to the center of the cluster. The Si atoms in the equatorial plane are ∼0.1 Å closer to each other, whereas they are ∼0.1 Å further from the capping Si atoms, as compared to the undoped cluster. Doping with B, however, causes a more substantial disruption of the geometric structure, since B is one row above Si, and it is much smaller. The B atom is substantially closer to the center of the cluster. It disrupts the positioning of the Si atoms in the equatorial plane. The adjacent Si atoms are pulled closer to the B atom and farther away from all other Si atoms. The remaining two equatorial Si's are farther from the remaining in-plane atoms, but are closer to the capping atoms. Thus, one can conclude that the equatorial B dopant creates a defect that extends over three atoms, due to the strong interaction between the B and the two nearest equatorial Si atoms. These observations are in line with the previous theoretical work on B and P doping in Si NCs, in which doping with B was found to cause a more substantial change to the geometry of the NC than did doping with P.[38]

The calculated optical absorption spectra are shown in Figure 2. The SAC−CI and linear response TDDFT results are presented next to each other for comparison. Linear response TDDFT is much less expensive computationally compared to SAC−CI. However, it remains within the single-particle description and attempts to include electron−hole interactions at the single-particle level by modification of the original Coulomb interaction potential. SAC−CI includes both SE and ME states. Overall, the SAC−CI and TDDFT spectra show similar features. The main peak appears at about the same energy. Because TDDFT contains only SE states, the total number of states in the SAC−CI spectra is an order of magnitude higher than that in the TDDFT spectra. This explains why the SAC−CI spectra contain additional peaks and a much denser manifold of states. The latter feature is critical not only for MEG but also for a proper treatment of electron−phonon relaxation at high energies.[39−41] Good qualitative agreement between the TDDFT and SAC−CI optical absorption spectra indicates that SE states carry the primary optical activity. At the same time, the energy spectrum at high energies is dominated by ME states, with SEs appearing occasionally among MEs.

Both SAC−CI and TDDFT show an apparent blue-shift of the spectra when Si_7 is doped with either phosphorus or boron. The peaks in the spectra shown in Figure 2 start appearing at higher energies in the doped systems. In large clusters, this effect is known as Pauli blocking.[11,12] The additional electron, donated into the CB by the P dopant, impedes excitations of VB electrons into the CB, causing a bleaching of the lowest exciton transitions. The reasoning for the B-doped cluster is similar. The lowest exciton transitions are bleached, since creation of a second hole in the VB is disfavored by the first hole generated from the p-type dopant.

As the size of the NCs decreases, this picture changes qualitatively. The impurity level goes deeper into the bandgap,

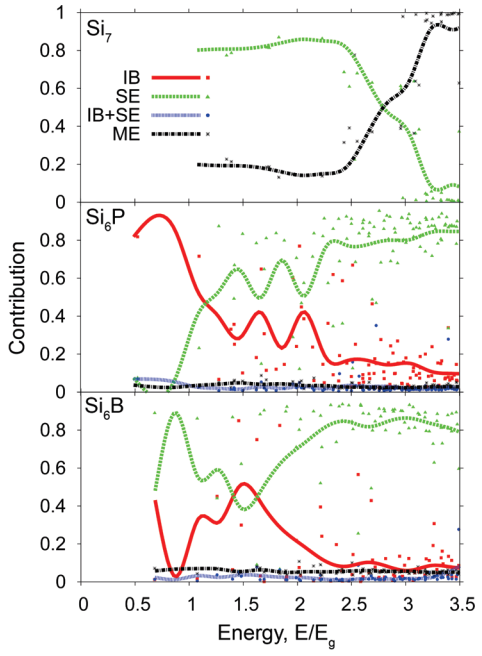

Figure 3. Contributions to the excited state character of the clusters from the different types of transitions shown in Figure 1, obtained with SAC−CI. The points are the squares of the expansion coefficients corresponding to the various transitions, whereas the lines give the average behavior. For clarity, only every fifth data point has been included in the plot.

and the dopant atom is no longer able to donate its charge to the CB or VB. In such a case, one expect a red shift in the spectrum due to absorption that occurs into the impurity state.[17,42] Our calculations do show that the impurity atoms introduce states within the bandgap. The data shown in Figure 3 start at much lower energies in the doped versus the pristine cluster. Whereas lower energy transitions do appear in the absorption spectra of the doped clusters, the intensity of these transitions is much smaller than the intensity of the transitions involving orbitals localized on the Si atoms. The vanishing oscillator strengths observed for the low-energy transitions are not attributed to the symmetric structure of the clusters. Other clusters with different degrees of symmetry studied in our group showed similar behavior upon charge-doping.[19,20] The small intensity of the low-energy transitions is rationalized by the overlap argument. The overlap, and therefore the transition dipole moment, between the impurity orbital localized on the dopant and the VB or CB orbitals delocalized over the rest of the cluster is smaller than the overlap between the VB and CB orbitals. Low-energy IB excited state configurations are clearly seen in Figure 3; however, they are eliminated from the spectra because their oscillator strengths are negligible.

Figure 3 shows the contributions of the different configurations to the excited state character. The configurations are defined in Figure 1. The lines in Figure 3 represent the average behavior of the data, whereas the symbols are the actual data points. For clarity, only every fifth data point is displayed in the figure, whereas the line is a running average over the entire data set. In the undoped cluster, the behavior is straightforward. SEs are the dominant configuration until ∼2.5 times the first excitation energy, at which point MEs become dominant. The relative energy of this switch between SEs and MEs is in agreement with what was measured in the experiments on undoped Si NCs.[32]

Addition of a dopant, such as B or P, has a noticeable effect on excited state character. As can be seen in Figure 3, the presence of the dopants shifts the threshold for pure MEs to much higher energies. In both doped clusters, the SE configuration is the main contributor for most of the energy window. The Si_6P cluster shows a heavy contribution from the IB configurations at low energies. It quickly fades as SEs take over. Pure SEs die off and MEs along with the IB + SE configurations start to rise at essentially the same rate only around $4E_g$. This energy is higher than the ionization threshold of the clusters, and, therefore, the corresponding data are not shown in the figures. The Si_6B cluster exhibits similar behavior, except for some minor differences. In particular, the IB configurations contribute less in the low-energy region, and the switch to the ME and IB + SE configurations occurs sooner, with the IB + SE configurations showing more contribution. The dopant atoms create large contributions, over 20%, to the lowest energy IB transitions, as should be expected. At the same time, they contribute less than 10% to the ME states near the MEG thresholds in the doped clusters.

Excitations at energies between $1E_g$ and $2E_g$ in the doped clusters are dark, even though they do show a substantial amount of SE character, as seen in the SAC−CI data in Figures 2 and 3. This indicates that strong optical transitions do not occur in the doped clusters until nearly twice the energy of the first excitation seen in the undoped cluster. If this result were to also be true for full-sized NCs, then doping could have a profound negative impact on the efficiency of photovoltaic devices. In particular, the yields of electron−hole pair generation by SE transitions would not be high due to the low optical activity of these transitions.

To ascertain whether the effects of the dopants on the electronically excited states of the clusters are dependent on dopant location, we repeated the calculations with the dopant atoms moved from their equatorial placement into an axial position. Figure 4 displays the results of these calculations. In this case, the SAC−CI and linear response TDDFT spectra show substantial differences at low energies. The SAC−CI data contain many optically active states that are absent in TDDFT. The corresponding spectra for the equatorially doped clusters are much more similar, Figure 2. Because SAC−CI is a more advanced approach than linear response TDDFT, one is led to conclude that at present the quality of TDDFT results depends on the location of the dopant. Optical activity in the SAC−CI spectra correlates with the rise of the SE excitations, as seen in the bottom panels in Figure 4. This should be expected because at the basic single particle level only one-electron excitations are optically allowed. Generally, linear response TDDFT should be able to match the SAC−CI results, as seen with the equatorial doping. The differences between the SAC−CI and TDDFT spectra observed in Figure 4 require further analysis.

Focusing on the SAC−CI results, one notices some minor differences in both the optical spectra and the contributions of the different configurations to the excited states of the equatorially and axially doped clusters, as seen in Figures 2 and 4, respectively. Nevertheless, the overall trends remain the same: a blue-shift in the optical spectra along with a shifting of multi-electron configurations to higher energies. Comparing the origin of the excited states, the only substantial difference between the equatorial and axial Si_6P clusters is in the low-energy behavior. The axial cluster shows a near even splitting of the IB and SE configurations before the SEs become dominant. Given the low optical activity in this energy range, the difference between the two clusters is unlikely to be significant. The axial Si_6B cluster

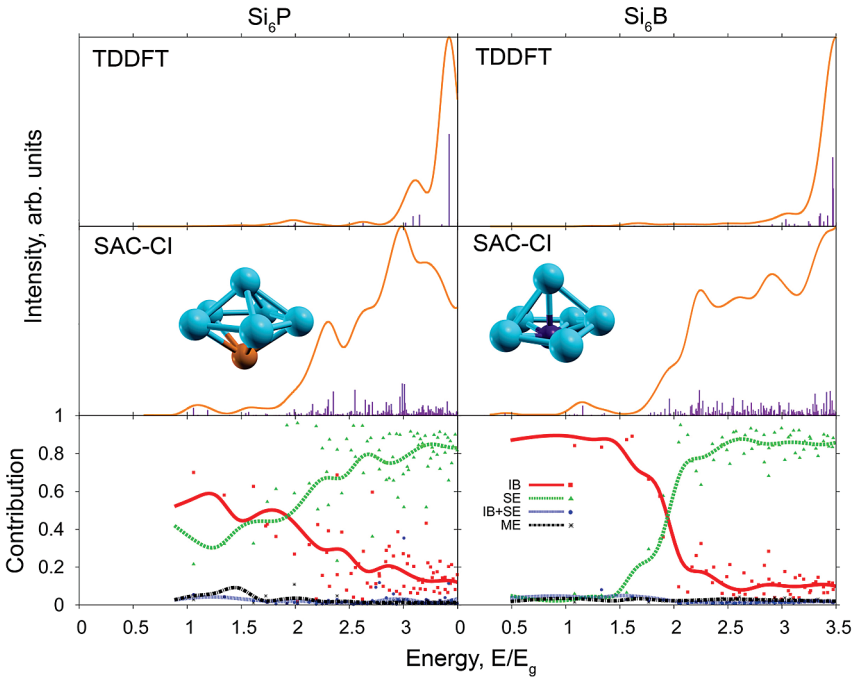

Figure 4. Calculated optical absorption spectra, optimized geometries, and excited state contributions for the dopant atoms in another position. The notation follows that in Figures 2 and 3. The bottom two panels are based on SAC−CI calculations.

also shows altered behavior at low energies. IB configurations have a more dominant role. This change is due to the bandgap in the axial Si_6B cluster being larger than that in the equatorial cluster. The larger energy gap allows the IB configurations to compete more favorably with the excitonic configurations. If this trend holds for larger systems, then the placement of boron dopants could be a significant factor in efficiency of MEG.[32−36]

The distinction between the IB and SE transitions made in this study emphasizes the fact that SE transitions create both an electron in the CB and a hole in the VB, whereas IB transitions generate only one charge carrier in the corresponding band, leaving the other carrier trapped at the dopant site. At high dopant concentrations, and when dopant states are close in energy to the VB or CB, the dopant sites create their own conductivity band. In such cases, one can redefine the band gap, referencing it with respect to the dopant band. Then, IB transitions become similar to SE transitions because they also create pairs of mobile charge carriers.

Generally, the changes in the excited state properties observed in the present study upon heterovalent doping are similar to the changes calculated for cluster charging.[19,20] This fact supports classification of charged clusters as doped.[11,36,43] It remains to be seen whether surface defects and ligands[44,41] induce similar changes to the nature and optical properties of high-energy electronic states in semiconductor NCs.

4. CONCLUSIONS

In summary, we performed sophisticated ab initio calculations on small semiconducting clusters to ascertain the effects of adding dopant atoms on the origin and optical activity of single and multiple excitons. These highest level calculations to date, in line with our previous work,[19,20,30] indicate that chemical modifications to the cluster disrupt the character of the excited states. New excited state configurations become possible either through the addition of a charge carrier into the VB or CB, or appearance of gap states. When dopant atoms are introduced, new IB transitions appear at low energies, whereas both optically active states and multielectron configurations shift to higher energies. Our clusters are ultrasmall[45,46] therefore, we cannot draw direct conclusions concerning larger NCs. We do expect that most of the current results should hold qualitatively for NCs as well. No matter the size of the system, dopant atoms create defect states inside the bandgap.[17,38] Optical or thermal excitations promote charge carriers residing in the gap states into the VB or CB. Because the changes to the excited state origin and optical absorption spectra seen here are due to these additional charge carriers, the effects calculated for the small clusters could be observed in full-sized NCs. Systematic experimental studies of these effects would be particularly valuable.

AUTHOR INFORMATION

Corresponding Author

*E-mail: oleg.prezhdo@rochester.edu.

ACKNOWLEDGMENT

The research was supported by NSF grant CHE-1050405.

REFERENCES

(1) Asahi, R.; Morikawa, T.; Ohwaki, T.; Aoki, K.; Taga, Y. *Science* **2001**, *293*, 269–271.
(2) Alivisatos, A. P. *Science* **1996**, *271*, 933–937.
(3) Mocatta, D.; Cohen, G.; Schattner, J.; Millo, O.; Rabani, E.; Banin, U. *Science* **2011**, *332*, 77–81.
(4) Dalpian, G. M.; Chelikowsky, J. R. *Phys. Rev. Lett.* **2006**, *96*, 226802.
(5) Chan, T. L.; Tiago, M. L.; Kaxiras, E.; Chelikowsky, J. R. *Nano Lett.* **2008**, *8*, 596–600.

(6) Bhargava, R. N.; Gallagher, D.; Hong, X.; Nurmikko, A. *Phys. Rev. Lett.* **1994**, *72*, 416–419.
(7) Wang, Y.; Herron, N.; Moller, K.; Bein, T. *Solid State Commun.* **1991**, *77*, 33–38.
(8) Schwartz, D. A.; Norberg, N. S.; Nguyen, Q. P.; Parker, J. M.; Gamelin, D. R. *J. Am. Chem. Soc.* **2003**, *125*, 13205–13218.
(9) Ochsenbein, S. T.; Feng, Y.; Whitaker, K. M.; Badaeva, E.; Liu, W. K.; Li, X. S.; Gamelin, D. R. *Nature Nanotechnol.* **2009**, *4*, 681–687.
(10) Bussian, D. A.; Crooker, S. A.; Yin, M.; Brynda, M.; Efros, A. L.; Klimov, V. I. *Nat. Mater.* **2009**, *8*, 35–40.
(11) Shim, M.; Wang, C. J.; Norris, D. J.; Guyot-Sionnest, P. *MRS Bull.* **2001**, *26*, 1005–1008.
(12) Shim, M.; Guyot-Sionnest, P. *Nature* **2000**, *407*, 981–983.
(13) Yu, D.; Wang, C. J.; Guyot-Sionnest, P. *Science* **2003**, *300*, 1277–1280.
(14) Perego, M.; Bonafos, C.; Fanciulli, M. *Nanotechnology* **2010**, *21*, 025602.
(15) Fujii, M.; Toshikiyo, K.; Takase, Y.; Yamaguchi, Y.; Hayashi, S. *J. Appl. Phys.* **2003**, *94*, 1990–1995.
(16) Norris, D. J.; Efros, A. L.; Erwin, S. C. *Science* **2008**, *319*, 1776–1779.
(17) Melnikov, D. V.; Chelikowsky, J. R. *Phys. Rev. Lett.* **2004**, *92*, 046802.
(18) Yang, C. S. *Microelectronics J.* **2008**, *39*, 1469–1471.
(19) Fischer, S. A.; Madrid, A. B.; Isborn, C. M.; Prezhdo, O. V. *J. Phys. Chem. Lett.* **2010**, *1*, 232–237.
(20) Isborn, C. M.; Prezhdo, O. V. *J. Phys. Chem. C* **2009**, *113*, 12617–12621.
(21) Nakatsuji, H.; Hirao, K. *J. Chem. Phys.* **1978**, *68*, 2053–2065.
(22) Nakatsuji, H.; Ehara, M. *J. Chem. Phys.* **1994**, *101*, 7658.
(23) Gaussian 03, Revision E.01. Frisch, M. J.; Trucks, G. W.; Schlegel, H. B.; Scuseria, G. E.; Robb, M. A.;Cheeseman, J. R.; Montgomery, Jr., J. A.; Vreven, T.; Kudin, K. N.; Burant, J. C.; Millam, J. M.; Iyengar, S. S.; Tomasi, J.; Barone, V.; Mennucci, B.; Cossi, M.; Scalmani, G.; Rega, N.; Petersson, G. A.; Nakatsuji, H.; Hada, M.; Ehara, M.; Toyota, K.; Fukuda, R.; Hasegawa, J.; Ishida, M.; Nakajima, T.; Honda, Y.; Kitao, O.; Nakai, H.; Klene, M.; Li, X.; Knox, J. E.; Hratchian, H. P.; Cross, J. B.; Bakken, V.; Adamo, C.; Jaramillo, J.; Gomperts, R.; Stratmann, R. E.; Yazyev, O.; Austin, A. J.; Cammi, R.; Pomelli, C.; Ochterski, J. W.; Ayala, P. Y.; Morokuma, K.; Voth, G. A.; Salvador, P.; Dannenberg, J. J.; Zakrzewski, V. G.; Dapprich, S.; Daniels, A. D.; Strain, M. C.; Farkas, O.; Malick, D. K.; Rabuck, A. D.; Raghavachari, K.; Foresman, J. B.; Ortiz, J. V.; Cui, Q.; Baboul, A. G.; Clifford, S.; Cioslowski, J.; Stefanov, B. B.; Liu, G.; Liashenko, A.; Piskorz, P.; Komaromi, I.; Martin, R. L.; Fox, D. J.; Keith, T.; Al-Laham, M. A.; Peng, C. Y.; Nanayakkara, A.; Challacombe, M.; Gill, P. M. W.; Johnson, B.; Chen, W.; Wong, M. W.; Gonzalez, C.; Pople, J. A.
(24) Dreuw, A.; Head-Gordon, M. *Chem. Phys.* **2005**, *104*, 4009.
(25) Levine, B. G.; Ko, C.; Quenneville, J.; Martinez, T. J. *Mol. Phys.* **2006**, *104*, 1039.
(26) Craig, C. F.; Duncan, W. R.; Prezhdo, O. V. *Phys. Rev. Lett.* **2005**, *95*, 163001.
(27) Isborn, C. M.; Li, X. *J. Chem. Phys.* **2008**, *129*, 204107.
(28) Giesbertz, K. J. H.; Pernal, K.; Gritsenko, O. V.; Baerends, E. J. *J. Chem. Phys.* **2009**, *130*, 114104.
(29) Turkowski, V.; Ullrich, C. A.; Rahman, T. S.; Leuenberger, M. N. *Phys. Rev. B* **2010**, *82*, 205208.
(30) Isborn, C. M.; Kilina, S. V.; Li, X.; Prezhdo, O. V. *J. Phys. Chem. C* **2008**, *112*, 18291–18294.
(31) Idrobo, J. C.; Halabica, A.; Magruder, R. H., III; Haglund, R. F., Jr.; Pennycook, S. J.; Pantelides, S. T. *Phys. Rev. B* **2009**, *79*, 125322.
(32) Beard, M. C.; Knutsen, K. P.; Yu, P. R.; Luther, J. M.; Song, Q.; Metzger, W. K.; Ellingson, R. J.; Nozik, A. J. *Nano Lett.* **2007**, *7*, 2506–2512.
(33) Mcguire, J. A.; Joo, J.; Pietryga, J. M.; Schaller, R. D.; Klimov, V. I. *Acc. Chem. Res.* **2008**, *41*, 1810–1819.
(34) Sewall, S. L.; Cooney, R. R.; Anderson, K. E. H.; Dias, E. A.; Sagar, D. M.; Kambhampati, P. *J. Chem. Phys.* **2008**, *129*, 084701.
(35) Rabani, E.; Baer, R. *Nano Lett.* **2008**, *8*, 4488–4492.
(36) Beard, M. C.; Midgett, A. G.; Law, M.; Semonin, O. E.; Ellingson, R. J.; Nozik, A. J. *Nano Lett.* **2009**, *9*, 836–845.
(37) Liu, B.; Lu, Z.-Y.; Pan, B.; Wang, C.-Z.; Ho, K.-M.; Shvartzburg, A. A.; Jarrold, M. F. *J. Chem. Phys.* **1998**, *109*, 9401–9409.
(38) Ossicini, S.; Iori, F.; Degoli, E.; Luppi, E.; Magri, R.; Poli, R.; Cantele, G.; Trani, F.; Ninno, D. *IEEE J. Sel. Top. Quant.* **2006**, *12*, 1585–1591.
(39) Kilina, S. V.; Craig, C. F.; Kilin, D. S.; Prezhdo, O. V. *J. Phys. Chem. C* **2007**, *111*, 4871–4878.
(40) Kilina, S. V.; Kilin, D. S.; Prezhdo, O. V. *ACS Nano* **2009**, *3*, 93–99.
(41) Hyeon-Deuk, K.; Madrid, A. B.; Prezhdo, O. V. *Dalton Trans.* **2009**, *45*, 10069–10077.
(42) Zurauskas, S.; Dargys, A.; Zurauskiene, N. *Phys. Status Solidi, B* **1992**, *173*, 647–660.
(43) Krauss, T. D.; Peterson, J. J. *J. Phys. Chem. Lett.* **2010**, *1*, 1377–1382.
(44) Kilina, S.; Ivanov, S.; Tretiak, S. *J. Am. Chem. Soc.* **2009**, *131*, 7717–7726.
(45) Evans, C. M.; Guo, L.; Peterson, J. J.; Maccagnano-Zacher, S.; Krauss, T. D. *Nano Lett.* **2008**, *8*, 2896–2899.
(46) Yang, P.; Tretiak, S.; Masunov, A. E.; Ivanov, S. *J. Chem. Phys.* **2008**, *129*, 074709.